Effect of Molecular Structure on the Thermodynamics of Block Copolymer Melts

C. C. Lin, S. V. Jonnalagadda, P. K. Kesani, H. J. Dai, and N. P. Balsara*

Department of Chemical Engineering, Polytechnic University, Six Metrotech Center, Brooklyn, New York 11201

Received June 2, 1994; Revised Manuscript Received August 16, 1994®

ABSTRACT: Small-angle neutron scattering profiles from linear polystyrene–polyisoprene block copolymers were measured as a function of temperature. Measurements were made on eight diblock copolymers and two triblock copolymers, with molecular weights ranging from 1.2×10^4 to 4.1×10^4 and ϕ ranging from 0.13 to 0.46 (ϕ is the volume fraction of the minor component). The scattering profiles were consistent with the mean-field theory of Leibler for block copolymers with $0.25 < \phi < 0.5$. Fluctuation corrections proposed by Fredrickson and Helfand were found to be increasingly important as the order–disorder transition was approached. However, large deviations between experiment and theory were observed in low molecular weight asymmetric block copolymers with $\phi < 0.25$. The amplitude of the concentration fluctuations was found to be an order of magnitude larger than predictions by Leibler, and Fredrickson and Helfand. These findings cannot be explained on the basis of a composition-dependent Flory–Huggins χ parameter because this anomaly is not evident in a higher molecular weight block copolymer with the same asymmetry (ϕ).

Introduction

There is considerable commercial and scientific interest in mixtures of unlike polymers. Theories based on the random phase approximation (RPA)[1–6] coupled with scattering experiments[7–10] have proven to be powerful for studying such systems. RPA theories assume a mean-field picture in which polymer–polymer interactions are characterized by the Flory–Huggins interaction parameter, χ.[11,12] Experimental scattering data obtained from polymer blends[7,8] and block copolymers[9,10] are in quantitative agreement with the RPA theory provided χ is treated as an adjustable parameter. Experimentalists have thus overwhelmingly adopted the RPA theory because vast amounts of scattering data can be compactly represented in terms of a few χ parameters.

However, the physics that underlies the measured χ parameters remains an important open question. In theory, the χ parameter is related to monomer–monomer interactions and thus should be independent of molecular weight and composition of the mixture. Several groups have measured the χ parameter in polymer blends as a function of composition and molecular weight. While χ parameters measured in binary polymer blends show no significant molecular weight dependence,[13–15] a persistent composition dependence has been observed.[13,16,17] Such studies demonstrate the limited applicability of the RPA and provide the motivation to pursue more detailed descriptions of polymer–polymer interactions.[18,19]

Much less is known about the molecular weight and composition dependence of χ parameters in block copolymer melts. Reported dependences of χ on temperature of polystyrene–polyisoprene block copolymers, for example, vary by over 100%[20–24] for reasons that are not well understood. Theoretical studies of Fredrickson and Helfand suggest that fluctuations in disordered block copolymers should cause substantial deviations from mean-field behavior.[25] Perhaps the observed variations in χ parameters is a manifestation of these effects. Experiments by Bates and co-workers[10] have substantiated some of the theoretical predictions of Fredrickson and Helfand. However, a systematic study of block copolymer thermodynamics as a function of molecular weight, composition, and temperature has not been conducted. Our objective in this paper is to identify the temperature, composition, and molecular weight range over which the mean-field theory is applicable in polystyrene–polyisoprene block copolymers. We have also attempted to explain departures from mean-field behavior. In particular, we have compared our data with predictions of the fluctuation theory of Fredrickson and Helfand[25] and Monte-Carlo simulations of Binder and Freid.[26,27]

This study concerns linear block copolymers and includes a symmetric and an asymmetric triblock copolymer in addition to a series of eight diblock copolymers.

Experimental Section

Polystyrene–polyisoprene diblock copolymers were synthesized by sequential anionic polymerization under high vacuum in a benzene/cyclohexane mixture, with *sec*-butyllithium as the initiator and 2-propanol as the terminator by sequential polymerization. Usually the shorter block was synthesized first. An aliquot of the reaction mixture containing these "living" anions was isolated and terminated before the addition of the second block. The molecular weight and polydispersity of the short block were obtained from GPC measurements on the precursor. The GPC was calibrated using polystyrene and polyisoprene standards. The composition of the block copolymers and the percentage of 1,2 addition in the polyisoprene block were obtained by ^{1}H NMR. The polyisoprene blocks in all the block copolymers were dominated by 1,4 addition (93–94%). A small amount (<0.5 wt %) of 2,6-di-*tert*-butyl-4-methylphenol was added to the block copolymer to inhibit degradation of the polyisoprene block. The polymers used in this study are listed in Table 1.

The polymers labeled SI(7–7), ISI(7–7–7), and ISI(7–7–15) represent a series of materials that were obtained from a single, three-step synthesis. A polyisoprene block with molecular weight of 7×10^3 g/mol was synthesized first, followed by the addition of the appropriate amount of styrene to give a symmetric diblock copolymer, SI(7–7). Roughly one-third of the reaction mixture was isolated and terminated with 2-propanol, and a predetermined amount of isoprene was then introduced into the reaction vessel to yield the symmetric

* To whom correspondence should be addressed.

® Abstract published in *Advance ACS Abstracts,* November 15, 1994.

0024-9297/94/2227-7769$04.50/0

Table 1. Characteristics of Polymers Used in This Study

sample desig	M_w of S block	M_w of I block(s)	vol. frac of S block	ODT temp[a] (°C)
SI(11−7)	11.3×10^3	6.6×10^3	0.60	121 ± 3
SI(6−6)	6.5×10^3	6.5×10^3	0.46	78 ± 1
SI(6−10)	5.6×10^3	9.9×10^3	0.33	NB
SI(6−13)	5.9×10^3	12.9×10^3	0.28	91 ± 2
SI(4−13)	4.2×10^3	12.6×10^3	0.22	59 ± 2
SI(8−22)	7.9×10^3	22.3×10^3	0.23	145 ± 2
SI(6−35)	6.0×10^3	35.3×10^3	0.13	NB
SI(7−7)	7.2×10^3	7.2×10^3	0.46	84 ± 1
ISI(7−7−7)	7.2×10^3	7.2×10^3 and 7.3×10^3	0.31	NB
ISI(7−7−15)	7.2×10^3	7.2×10^3 and 15.5×10^3	0.22	NB

[a] Samples that were not birefringent in the observable temperature window are labeled NB.

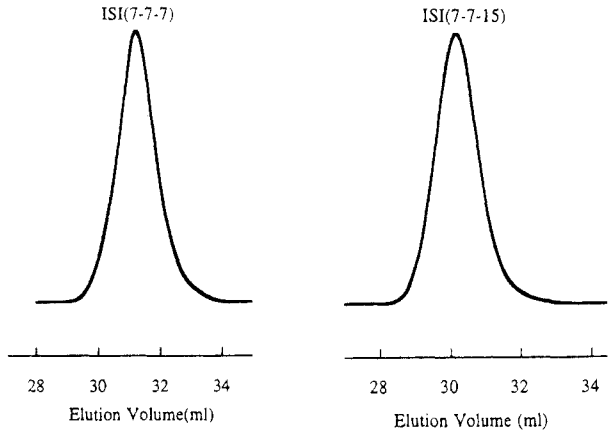

Figure 1. Typical GPC traces of the block copolymers used in this study.

triblock copolymer. Roughly half of the reaction mixture was then isolated and terminated to give ISI(7−7−7), and the appropriate amount of isoprene was added and polymerized to give ISI(7−7−15). All the operations were carried out in a single, all-glass, sealed apparatus under high vacuum; the appropriate amounts of the required materials were attached via break seals to the reactor. The GPC traces of the triblock copolymers are shown in Figure 1 and are typical of materials used in this study.

The polydispersities of the precursor as well as the block copolymer were less than 1.1. All the materials were used as synthesized; no fractionation was required. The order−disorder transition in these materials was determined by the birefringence method using an apparatus and procedure described in refs 28 and 29. The important characteristics of the block copolymers used in this study are given in Table 1.

Small-angle neutron scattering (SANS) experiments on melts of these polymers were conducted over a range of temperatures (27−172 °C). Only data above the glass transition temperatures of the materials are discussed in this paper. Two-dimensional SANS patterns were obtained from 1 mm thick samples held within quartz windows on the 8 m SANS machine (on the NG5 beam line) at the National Institute of Standards and Technology (NIST) at Gaithersburg, MD. The following instrument configuration was used: neutron wavelength $\lambda = 9.0$ Å, wavelength spread $\Delta\lambda/\lambda = 0.25$, sample-to-detector distance = 3.6 m, sample aperture = 1.2 cm, source-to-sample distance = 4.5 m, and source size = 2.7 cm. Reasonable scattering intensities were obtained from the samples due to the natural neutron contrast between polystyrene and polyisoprene; no deuterium labels were used. Measurement times required for acquiring each scattering profile ranged between 10 and 30 min, depending on the proximity to the ODT. The scattering data were corrected for background, empty cell scattering, and detector sensitivity, converted to an absolute scale using secondary standards provided by NIST, and azimuthally averaged. The absolute intensity

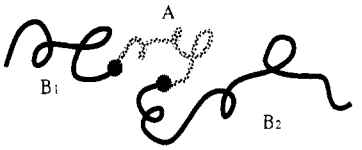

Figure 2. Schematic representation of an asymmetric B_1−A−B_2 triblock copolymer, where B_1 and B_2 are chemically identical blocks differing only in molecular weight.

calibration was verified using secondary standards developed by the Exxon/Princeton group[30] as well as standards developed by the Polytechnic group.[31] The incoherent scattering, I_{inc}, for each of the block copolymers was estimated from SANS measurements on a pure poly(methylbutylene) homopolymer, assuming that it is proportional to the concentration of H atoms in the copolymer, and subtracted from the azimuthally averaged scattering profiles to give the coherent scattering intensity, $I(q)$ ($q = 4\pi \sin(\theta/2)/\lambda$, where θ is the scattering angle).[32] The coherent scattering intensity is thus obtained from the raw data without resorting to any adjustable parameters.

Mean-Field Theory

We derive an expression for the scattering from a triblock copolymer, depicted in Figure 2, in which the two outer blocks are chemically identical but differ in molecular weight. All the materials examined in this paper may be considered as special cases of this general architecture (see Table 1). The incompressible, multicomponent RPA formalism of Akacsu et al.,[6] which is a generalization of the pioneering work of de Gennes[1] and Leibler,[2] provides a convenient framework for the derivation. Many features of the formalism of Akcasu et al. are contained in an early publication by de Gennes[3] in which he derived the scattering function of a ring, multiblock copolymer. Multicomponent RPA, when applied to a B_1−A−B_2 triblock copolymer, gives the following expression for the coherent scattered intensity, $I(q)$:

$$I(q) = \left(\frac{b_A}{v_A} - \frac{b_B}{v_B}\right)^2 \{S_{11} + S_{22} + 2S_{12}\} \qquad (1)$$

Subscripts A and B refer to the two chemically distinct monomers in the copolymer, while subscripts 1 and 2 refer to the B blocks, B_1 and B_2, respectively (see Figure 2). The symbols b_i and v_i represent the scattering lengths and volumes of the monomers, respectively, and S_{ij} are components of a 2 × 2 structure factor matrix, **S**. The A block is treated as the "invisible" component (eliminated due to incompressibility), and thus only correlations between the B blocks are relevant. The structure factor matrix is evaluated as follows:

$$\mathbf{S} = \left[(\mathbf{S}^\circ)^{-1} + \frac{\underline{Y}\,\underline{Y}^T}{S_{AA}^\circ - m} - \frac{2\chi_m}{v}\mathbf{U}\right]^{-1} \qquad (2)$$

We use the symbol χ_m to represent the mean-field Flory−Huggins parameter, which is based on a reference volume, v. **U** is a 2 × 2 matrix in which each element is unity.

The components of matrix $\mathbf{S}^\circ$ and the scalar S_{AA}° in eq 2 are "ideal" partial structure factors and describe intramolecular correlations in the absence of interactions ($\chi_m = 0$). The diagonal components of $\mathbf{S}^\circ$ are the partial structure factors of blocks B_1 and B_2, while S_{AA}° is the partial stucture factor of the A block.

$$S_{ii}^\circ = \phi_i N_i v_i P_i(q) \qquad (i = 1, 2, A) \qquad (3)$$

The off-diagonal components of $\mathbf{S}^\circ$ are related to interblock correlations between blocks B_1 and B_2.

$$S_{12}^\circ = S_{21}^\circ = (\phi_1 N_1 \phi_2 N_2)^{1/2} v_B F_1(q) E(q) F_2(q) \quad (4)$$

In eqs 3 and 4, N_i is the number of monomers in block i and ϕ_i is its volume fraction. Functions $P_i(q)$ and $F_i(q)$ describe the intrablock and interblock correlations, while $E(q)$ describes correlations between the two A–B junctions in the copolymer. For Gaussian chains, functions $P_i(q)$, $F_i(q)$, and $E(q)$ are given by[1,2,33]

$$P_i(q) = 2\frac{\exp(-x_i) - 1 + x_i}{x_i^2} \quad (i = 1, 2, A) \quad (5)$$

$$F_i(q) = \frac{1 - \exp(-x_i)}{x_i} \quad (i = 1, 2, A) \quad (6)$$

$$E(q) = \exp(-x_A) \quad (7)$$

where $x_i = q^2 N_i l_i^2/6$ and l_i is the statistical segment length of species i.

The vector $\underline{Y}$ in eq 2 is given by

$$\underline{Y} = (\mathbf{S}^\circ)^{-1}\underline{S}_A^\circ + \underline{I} \quad (8)$$

where the vector $\underline{S}_A^\circ$ describes ideal correlations between block A and the two B blocks, 1 and 2

$$S_{Ai}^\circ = (\phi_A N_A v_A \phi_i N_i v_B)^{1/2} F_A(q) F_i(q) \quad (i = 1, 2) \quad (9)$$

and $\underline{I}$ is the identity vector.

The scalar quantity m in eq 2 is given by

$$m = (\underline{S}_A^\circ)^T (\mathbf{S}^\circ)^{-1} (\underline{S}_A^\circ) \quad (10)$$

If the molecular weight of one of the B blocks is set to zero and the appropriate correlations are ignored, then eq 1 reduces to Leibler's result for an A–B diblock copolymer[2]

$$I(q) = \left(\frac{b_A}{v_A} - \frac{b_B}{v_B}\right)^2 \left\{\frac{S_{AA}^\circ + S_{BB}^\circ + 2S_{AB}^\circ}{S_{AA}^\circ S_{BB}^\circ - (S_{AB}^\circ)^2} - \frac{2\chi_m}{v}\right\}^{-1} \quad \text{(diblock)} \quad (11)$$

The subscripts 1 and 2 are now unnecessary and have been replaced by B, the "ideal" structure factors S_{ii}° are given by eq 3, and S_{AB}° can be gotten from eq 9 by replacing subscript i by B.

Other derivations of the scattered intensity from triblock copolymers have been worked out by Mayes and Olvera de la Cruz[34] and Mori et al.[35]

Birefringence Determination of the Order–Disorder Transition

All the theories on block copolymer thermodynamics discussed in this paper are restricted to systems that are single-phase and disordered. To obtain thermodynamic information from scattering profiles, we thus must ensure that the sample is disordered. We have used the birefringence method[28,29,36] to determine the temperature range over which each polymer is disordered. The fraction of incident light transmitted through the sample held between crossed polarizers, P/P_0 (P is the transmitted power, and P_0 is the incident power of a He–Ne laser) was measured as a function of temperature. It was shown if the sample is ordered and consists of randomly oriented uniaxial grains, then P/P_0 is given by[29,37]

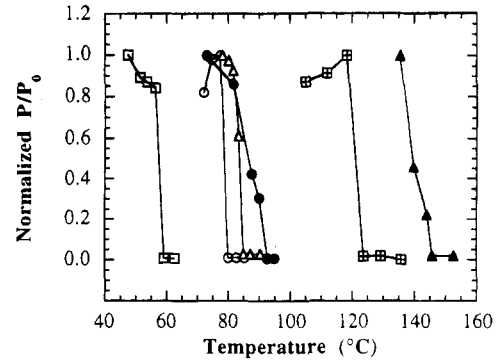

Figure 3. Dependence of birefringence (P/P_0) on temperature for several block copolymers. The data are divided by a constant (norm) so that they can be shown on the same plot (actual P/P_0 = normalized P/P_0 × norm). The values of norm for each polymer are given in square brackets: open squares, SI(4–13) [2.53×10^{-2}]; open circles, SI(6–6) [2.55×10^{-2}]; open triangles, SI(7–7) [2.87×10^{-2}]; filled circles, SI(6–13) [5.27×10^{-2}]; hatched squares, SI(11–7) [4.27×10^{-2}]; filled triangles, SI(8–22) [1.39×10^{-2}].

$$\frac{P}{P_0} = \frac{4\pi^2}{15}(\Delta n)^2 \frac{L l_{av}}{\lambda^2} \quad (12)$$

where Δn is the difference in refractive index for light polarized parallel and perpendicular to the optical axis of a single grain, L is the sample thickness (path length of the beam), l_{av} is the characteristic size of the grains, and λ is the wavelength of the light. The birefringence of disordered materials must be zero (or nearly so).[25,26,31,32] Thus the order–disorder transition (ODT) can be identified as the temperature at which (P/P_0) decreases to zero.

Plots of P/P_0 versus temperature for six of the block copolymers—SI(11–7), SI(6–6), SI(6–13), SI(4–13), SI(8–22), and SI(7–7)—are shown in Figure 3. A singularity in the birefringence data is evident in all of the materials. P/P_0 values obtained from the other polymers were essentially zero over the entire observable temperature window, indicating that these samples were disordered.

The ODT results are summarized in Table 1.

This method of assigning the ODT's is consistent with current theories.[2,25] In Leibler's mean-field theory, the ordered phase formed when a block copolymer crosses the stability limit, i.e., the spinodal point, is always cylindrical (except when ϕ exactly equals $^1/_2$).[2] The fluctuation theory, on the other hand, predicts the formation of metastable cylindrical or lamellar phases upon entering the ordered region for low molecular weight block copolymers ($N = 10^4$).[25] Fluctuation corrections suppress the spinodal point to $T = 0$ K.[25] Since both cylindrical and lamellar phases have finite Δn,[38] the birefringence discontinuity can be interpreted as either the location of the spinodal on the basis of the mean-field theory or the limit of metastability on the basis of the fluctuation theory.

If, on the other hand, these theories are incorrect and phases with cubic symmetry ($\Delta n = 0$) are formed upon entering the ordered region, then the ODT would not be accompanied by a decreased birefringence. Recently, Bates and co-workers have identified a spherical-to-disordered transition in a polyolefin diblock copolymer.[41] The SANS data that we present in the following sections

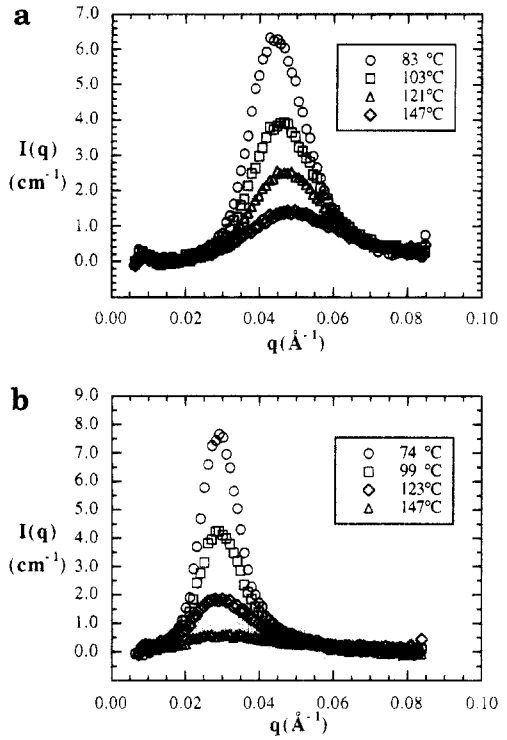

Figure 4. SANS profiles obtained from (a) SI(6−6) and (b) SI(6−35) at selected temperatures.

confirm that, for the polymers examined in this study, the discontinuous decrease in birefringence occurs due to disordering.

Alternative methods for locating the ODT in block copolymers include rheology[10,39,40] and small-angle scattering from shear-oriented materials.[10] In previous work it has been demonstrated that the ODT measured by the birefringence method is consistent with these techniques.[28,36,42,43]

Position of the Scattering Maximum

In Figure 4a we show SANS data obtained from a symmetric diblock copolymer, SI(6−6), and in Figure 4b we show SANS data obtained from an asymmetric block copolymer, SI(6−35). The qualitative features of both scattering curves are similar and representative of data obtained from all the materials. We see a well-defined peak at low temperatures, which diminishes in intensity as temperature increases. Roe and co-workers first made this observation.[44] Note the scattered intensity decays to zero (within experimental error) in both high-q and low-q limits, as expected from theory.[1,2] This is a measure of accuracy of the instrument calibration and background subtraction procedures. These features were observed in diblock as well as triblock copolymers.

In Figure 5 we plot q_m versus temperature and find that all the block copolymers behave similarly in the accessible temperature range. The peak position shifts to higher values of q with increasing temperature. Notice that we have included some data obtained from ordered systems (see caption of Figure 5), and the values of q_m obtained from these systems are in close agreement with extrapolations from the disordered state. In all cases, the dependence of q_m on T can be approximated by a straight line:

$$q_m = AT + B \tag{13}$$

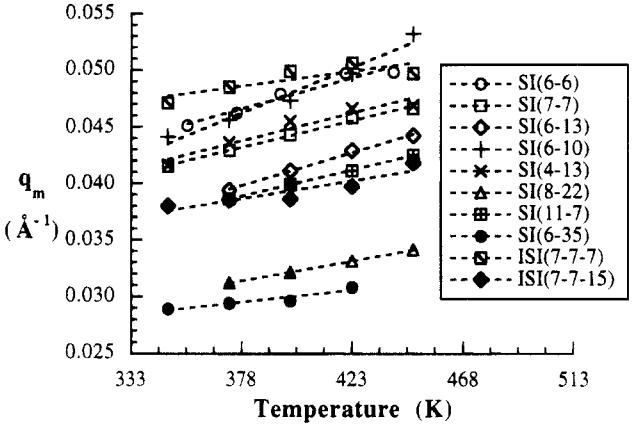

Figure 5. Dependence of q_m, the scattering vector at the peak, on temperature for all block copolymers. The solid squares and the solid triangles represent data obtained from SI(11−17) and SI(8−22) in the ordered state. All other data were obtained in the disordered state. The dashed lines represent least-squares fits through each data set.

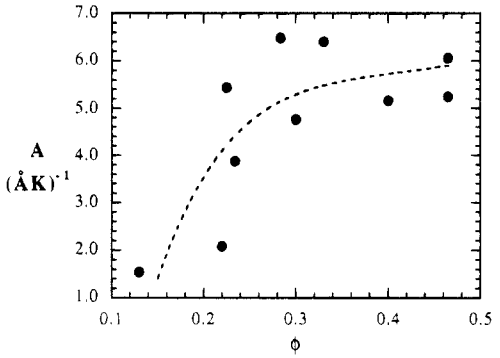

Figure 6. Dependence of A, the slope of the q_m versus T straight lines, versus ϕ, the volume fraction of the minor component.

The slopes of these straight lines are given in Figure 6, where we plot A versus ϕ. For most of the copolymers, A scatters around 5 (Å K)$^{-1}$. However, the most asymmetric copolymers, SI(6−35) and ISI(7−7−15), show lower values of about 2 (Å K)$^{-1}$.

The presence of a small-angle scattering maximum from disordered block copolymers was predicted by RPA theory and is a consequence of connectivity of the blocks.[1,2] The location of the maximum in q-space, q_m, is related to the spatial extent of the concentration fluctuations in the distorted state and is predicted to depend mainly on the composition and molecular weight of the block copolymer.[2] For a series of diblock copolymers consisting of the same chemical species A and B but with different N_i and ϕ_i, the mean-field theory[2] predicts

$$q_m R_g = c(\phi) \tag{14}$$

where R_g is the radius of gyration of the chains, $c(\phi)$ is an order 1 constant that depends only on the composition of the block copolymer, and ϕ is the volume fraction of the minor component. It is our purpose to perform a stringent test of eq 14. The materials at our disposal allowed us to test the concentration, temperature, and molecular weight dependence of $c(\phi)$. Since $R_g \sim N^{1/2}$ (where N is the total number of repeat units in the block copolymer), it follows from eq 14 that the product $q_m N^{1/2}$ should also be only a function of ϕ. The advantage of plotting $q_m N^{1/2}$ (instead of $q_m R_g$) versus ϕ is that all three quantities, q_m, N, and ϕ, are obtained directly from

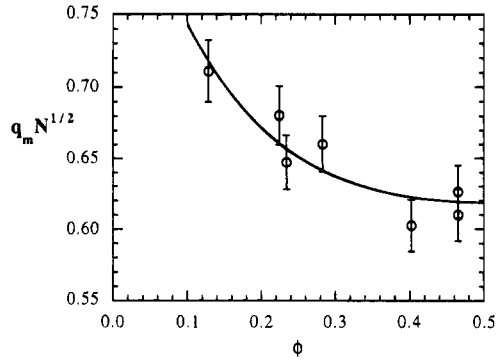

Figure 7. Plot of $q_m N^{1/2}$ versus ϕ for all of the diblock copolymers at 147 °C. The solid curve represents the mean-field theory shifted vertically so that agreement is forced at $\phi = 0.5$.

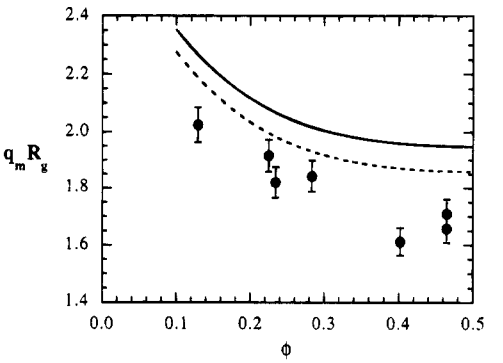

Figure 8. Plot of $q_m R_g$ versus ϕ for all of the diblock copolymers at 147 °C, where R_g is based on homopolymer chain dimensions. The solid curve represents the mean-field theory for monodisperse block copolymers. The dashed curve represents the mean-field theory for block copolymers with a Zimm–Schulz distribution and a polydispersity index of 1.05 for each block.

experimental data, q_m from SANS, N from GPC and NMR, and ϕ from NMR; no additional information or data fitting is required. In Figure 7 we plot $q_m N^{1/2}$ versus ϕ for all of the diblock copolymers at 147 °C. The number of repeat units per chain, N, is based on a reference volume of 150.3 Å^3 (see Nomenclature section). Some of the block copolymers are close to the ODT at 147 °C, while others are far away. For instance, SI(4–13) and SI(8–22) have nearly identical composition ($\phi = 0.23$) but SI(4–13) is 95 °C above its ODT while SI(8–22) is only 2 °C above the ODT. Nevertheless, the data from all the block copolymers collapse onto a single curve when plotted according to Leibler's suggestion. Considering the wide range of q_m (0.03–0.05 Å^{-1}), N (150–500), and ϕ (0.13–0.46) covered, this collapse represents a significant simplification.

The solid line in Figure 7 represents Leibler's prediction. The proportionality constant between R_g and $N^{1/2}$ was adjusted so that the theory and experiment were in agreement at $\phi = 0.5$. It is evident that the observed dependence of $q_m N^{1/2}$ on ϕ is consistent with the prediction of Leibler. This proportionality constant can be interpreted as a composition-independent, average statistical segment length for SI block copolymers at 147 °C. This average statistical segment length is equal to 7.7 Å. To a very good approximation, the theoretical curve in Figure 7 is given by

$$q_m N^{1/2} = 0.618 + 0.36(\phi - 0.5)^2 + 2.64(\phi - 0.5)^4 \quad (15)$$

The unperturbed dimensions of homopolystyrene and homopolyisoprene chains are well known. We can thus estimate the unperturbed dimensions of the block copolymers, R_g, assuming that they can be represented as concatenated random walks:

$$R_g = (R_{g,S}^2 + R_{g,I}^2)^{1/2} \quad (16)$$

where $R_{g,S}$ and $R_{g,I}$ are the radii of gyration of the individual polystyrene and polyisoprene blocks, respectively, if they were homopolymers. Fetters and coworkers have conducted extensive studies on the unperturbed dimensions of homopolymers, and their most recent studies suggest that $R_g/M^{1/2}$ for polystyrene and polyisoprene homopolymers is 0.268 and 0.332 (Å mol$^{1/2}$/g$^{1/2}$), respectively, at 140 °C (M is the molecular weight of the homopolymers).[45] Using these values, the R_g of all the block copolymers were computed and the product $q_m R_g$ is plotted versus ϕ in Figure 8, along with Leibler's explicit prediction (solid curve). Neither the theoretical curve nor the experimental data are shifted. It is apparent that the extent of fluctuations ($1/q_m$) is systematically larger than that predicted by Leibler. Some of this discrepancycan be attributed to polydispersity effects. The effect of polydispersity on scattering from diblock copolymers has been examined by Leibler and Benoit,[46] Benoit et al.,[47] and Burger et al.[48] wherein each block has a Zimm–Schulz distribution. The theoretical result for block copolymers in which each of the blocks has a polydispersity index of 1.05 is shown by the dashed curve in Figure 8.

The Mean-Field Flory–Huggins Interaction Parameter

The shape of the observed scattering profiles was found to be in good agreement with the mean-field predictions.[2,6] In Figure 9a we compare experimentally measured scattering data from SI(7–7) with the mean-field theory—eq 11—using χ_m and l_i as adjustable parameters. The heights of the theoretical and experimental curves were matched by adjusting χ_m. The statistical segmental lengths of the blocks, l_A and l_B, were chosen so that the experimental and theoretical values of q_m were in agreement. However, several combinations of l_A and l_B satisfy this criterion. In this work we use a single statistical segment length to describe the two blocks; i.e., $l = l_A = l_B$. We repeated our procedure for estimating χ_m and found that the estimates of χ_m were unaffected by the choice of l_A and l_B. Thus the shape of the scattering curves is gauged by two parameters, χ_m, which is related to the height of the scattering peak, and l, which is related to the position of the scattering peak. All the other parameters required to compute predictions of the mean-field theory (see eq 11) were estimated from characterization data and are summarized in Appendix 1.

As is evident from Figure 9a, there is quantitative agreement between theory and experiment at high temperatures. However, at lower temperatures the theoretical curves are systematically narrower than the experimental data. This was found to be true for all of the block copolymers and is due to instrumental smearing. The effect of smearing is examined in Appendix 2, where it is shown to have a negligible effect on our estimate of χ_m and l (<1%).

In parts b and c of Figure 9 we compare experimental data obtained from the two triblock copolymers with the mean-field theory[6]—eqs 1–10—again with only χ_m and l as adjustable parameters. We find that the RPA

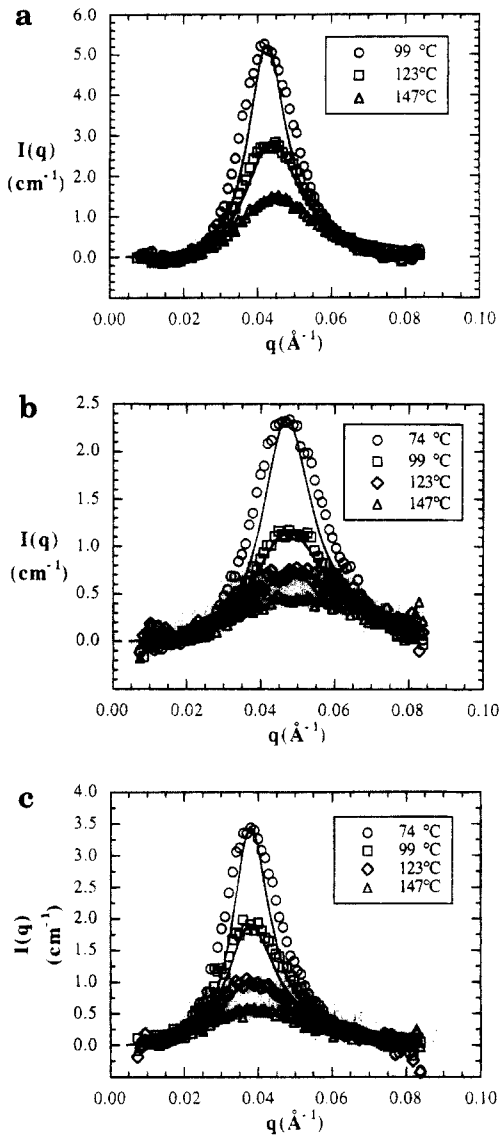

Figure 9. Typical agreement between measured SANS profiles and mean-field theory, using χ_m and l as adjustable parameters: (a) SI(7−7); (b) ISI(7−7−7); (c) ISI(7−7−15).

applies equally well to ISI(7−7−7) and ISI(7−7−15), in spite of their architectural complexity. It is interesting to note that scattering peaks obtained from the asymmetric triblock—ISI(7−7−15)—are much sharper than those obtained from the symmetric triblock—ISI(7−7−7). This effect is evident in both the experimental data and the predictions of the mean-field theory. This implies that the length scale of the concentration fluctuations in ISI(7−7−15) is more sharply defined than that in ISI(7−7−7). This is somewhat counterintuitive because one expects the inequality of the lengths of the polyisoprene blocks in ISI(7−7−15) to lead to greater disorder, i.e., broader peaks. This effect would not be surprising if ISI(7−7−15) were nearer to the ODT than ISI(7−7−7). However, as discussed later in the section on scattering near the ODT, this is not the case.

The dependence of the mean-field Flory−Huggins interaction parameter χ_m on temperature T is depicted in Figure 10, where we plot χ_m as a function of $1/T$ for all of the polymers listed in Table 1. All the χ values reported in this paper are based on a reference volume of 150.3 Å^3, which is the geometric mean of the monomer volumes of polystyrene and polyisoprene at 80 °C. If the measured χ parameters were in perfect agreement with the Flory−Huggins theory and if there were no

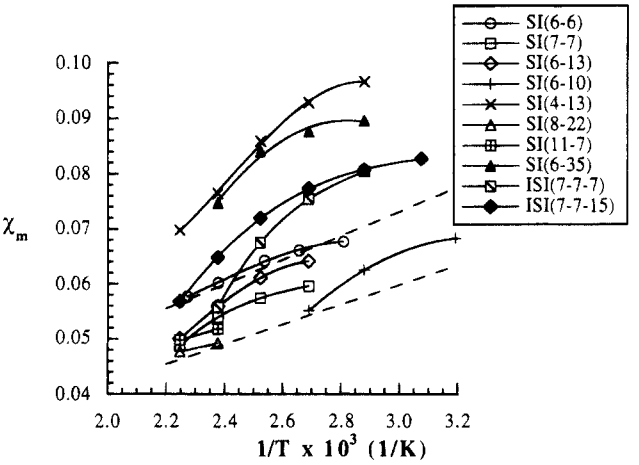

Figure 10. Dependence of χ_m, the mean-field χ parameter, on $1/T$ for all of the block copolymers. The dashed lines represent eq 17 with ±10% uncertainty.

experimental errors, then all the data would have collapsed onto a single line. We, however, find considerable scatter in the data. Experimental uncertainty, due mainly to errors in estimation of N_i and instrument calibration, can account for deviations of about 10%. The observed deviations are in the vicinity of 100% and thus well outside experimental uncertainty. These deviations imply a breakdown of the mean-field theory unless we accept the feeble hypothesis that the Flory−Huggins χ parameter has a significant molecular weight and composition dependence.

The Flory−Huggins theory anticipates a linear dependence of χ on $1/T$. In contrast, we find a systematic, negative curvature in the χ_m versus $1/T$ plots (Figure 10). This nonlinearity is, perhaps, another indication of the failure of the mean-field theory. Since the parameter χ_m is a measure of the height of the scattering peak, the curvature in the χ_m versus $1/T$ data indicates that the increase in the height of the scattering peak with decreasing temperature occurs at a rate that is slower than that predicted by the mean-field theory.

In spite of the inadequacies of the mean-field theory, we find some systematic trends. The curvature in the χ_m versus $1/T$ data is most prominent in SI(4−13), SI(6−35), ISI(7−7−7), and ISI(7−7−15). The feature common to this group is that they are highly asymmetric in composition, with $\phi < 0.25$. If we choose to focus on the block copolymers with $0.25 < \phi < 0.5$, we find two rather significant simplifications. First, we find that the curvature in the χ_m versus $1/T$ data is small. Second, the data can be reasonably described by the following straight line:

$$\chi_m = 0.0064 + \frac{20.0}{T} \quad (\pm 10\%) \qquad (17)$$

which is in reasonable agreement with some of the reported dependences of χ on T[23,24,28] but not with others.[21,22]

The dashed lines in Figure 10 represent eq 17 with 10% uncertainty. It is evident that the data from block copolymers with compositions in the mid range are in reasonable agreement with the mean-field theory. However, predictions based on eq 17 can lead to large errors if applied to highly asymmetric block copolymers. For example, eq 17 would predict $I_m = 0.26$ cm^{-1} for SI(4−13) at 75 °C. We find experimentally that I_m is 4.0 cm^{-1}, which is an order of magnitude larger.

There also appears to be an interesting molecular weight effect. SI(4−13) and SI(8−22) are polymers with nearly identical compositions but differ in molecular weight by a factor of 2. In contrast to the data obtained from SI(4−13), we find that χ_m obtained from the block copolymer with the higher molecular weight—SI(8−22)—is consistent with eq 17. The applicability of the mean-field theory thus seems to depend on both composition and molecular weight: symmetric architectures and higher molecular weights lead to better agreement between experiment and theory.

Equation 17 provides a convenient "baseline" for cataloguing departures from mean-field behavior. All the block copolymers that exhibit departures from mean-field behavior give χ_m values that are larger than those given by eq 17. This implies that the amplitude of the fluctuations in these materials is larger than that predicted by the mean-field theory. Furthermore, χ_m values of the block copolymers with $\phi < 0.25$ are seen to approach eq 17 at higher temperatures. There thus appears to be a general trend toward mean-field behavior at higher temperatures.

The data that we have obtained are quite different from those reported by Stuhn for polystyrene−polyisoprene diblock copolymers.[22] For materials similar in molecular weight and composition to those studied by us, Stuhn found no curvature in the χ_m versus $1/T$ plots. He also found that χ_m values from an asymmetric block copolymer that closely resembled SI(4−13) were lower than those obtained from a symmetric block copolymer that resembled SI(6−6).

The consistency between the χ_m values obtained from both the triblock copolymers ISI(7−7−7) and ISI(7−7−15) at all temperatures provides a substantial confirmation of the multicomponent RPA formalism.[3−6,33] In fact, at high temperatures we observe quantitative agreement between triblock and diblock χ_m parameters. At lower temperatures the triblock χ_m values deviate from eq 17. Both SI(6−13) and ISI(7−7−7) have similar values of composition and molecular weight, yet SI(6−13) is more or less consistent with eq 17 while ISI(7−7−7) is not. Triblock copolymers are thus more susceptible to deviate from mean-field behavior than diblock copolymers with identical composition and molecular weight. However, we cannot attribute the observed deviations entirely to architectural differences between diblock and triblock copolymers because larger deviations are observed in the asymmetric diblocks—SI(4−13) and SI(6−35).

The limited applicability of the RPA-based equations forces us to go beyond the mean-field theory to explain our results.

Fluctuation Corrections to the Flory−Huggins Interaction Parameter

The importance of fluctuations in block copolymers was recognized by Leibler.[2] He commented that block copolymers belong to a universal class of fluctuating materials that were comprehensively analyzed by Brazovskii.[49] Fredrickson and Helfand applied the Brazovskii theory to diblock copolymers[25] and predicted substantial corrections to the mean-field theory. They found that the Leibler result—eq 11—could still be used to describe disordered block copolymers provided the parameter χ_m is considered to be a quantity that was indirectly related to the mean-field Flory−Huggins χ. They provide an explicit relationship between χ_m and χ, and thus the data shown in Figure 10 can be directly recast into Flory−Huggins interaction parameters. No reanalysis of the scattering profiles is necessary. We refer to the χ parameter extracted from the scattering data using the Fredrickson−Helfand theory[25] as a fluctuation-corrected χ, χ_f.

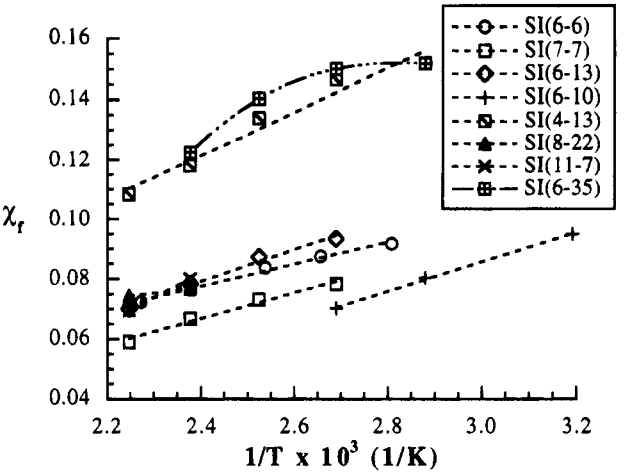

Figure 11. Dependence of χ_f, the χ parameter corrected for fluctuation effects, on $1/T$ for all of the diblock copolymers. χ_f values obtained from SI(6−6), SI(6−13), SI(8−22), and SI(11−7) at high temperatures are nearly identical.

The relationship between χ_f and χ_m is given by[10,25]

$$\chi_f = \chi_m + \frac{C(\phi)v}{2l^3N^2}\left\{\frac{F(x^*,\phi)}{N} - 2\chi_m\right\}^{-1/2} \qquad (18)$$

where the quantities C, l, N, F, and x^* can be calculated using the characterization and SANS data from each block copolymer. Thus, one can account for fluctuations without resorting to any additional parameters. Details concerning the calculation of χ_f from χ_m are given in Appendix 3.

In Figure 11 we plot χ_f as a function of $1/T$ for all of the diblock copolymers. We have not included the triblock data. Fluctuation corrections in triblock copolymers have been considered.[50] However, we were unable to find a simple way to apply the results of these calculations to our data. The linearity of the χ_f versus $1/T$ plots is the most remarkable difference between the fluctuation theory results and those obtained from the mean-field theory (compare Figures 10 and 11). This linearity is observed over a wide range of molecular weights and composition. Thus the observed curvature of χ_m versus $1/T$ data can be attributed to fluctuation effects. Bates and co-workers first observed this effect in a polyolefin diblock copolymer.[10] Only data from SI(6−35) show definite curvature. The data from most of the copolymers are consistent with the following straight line:

$$\chi_f = 0.0118 + \frac{26.5}{T} \quad (\pm 10\%) \qquad (19)$$

Equation 19 works rather well for all the diblock copolymers with $0.25 < \phi < 0.5$, regardless of molecular weight. For $\phi = 0.23$, we see that the fluctuation theory does provide a value for χ_f that is consistent with eq 19 for the higher molecular weight species—SI(8−22)—but not for the lower molecular weight species—SI(4−13).

Hence both the mean-field and fluctuation theories break down when applied to low molecular weight, asymmetric diblock copolymers. Difficulties in developing theories for such molecules were anticipated in a

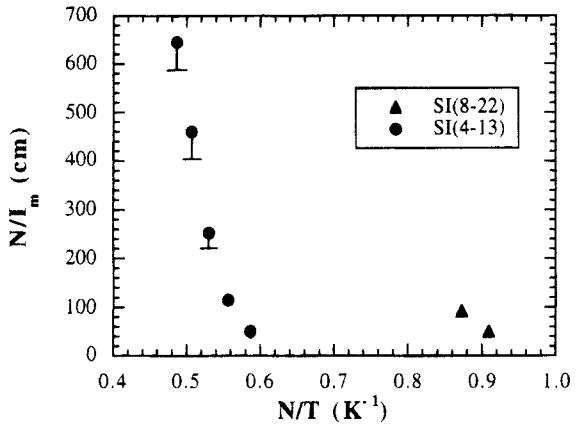

Figure 12. Plot of N/I_m versus N/T for block copolymers with $\phi = 0.23$. The solid symbols represent the measured I_m, and the lower limit of the error bar represents the calculated peak intensity after the effect of instrumental smearing has been considered (see Appendix 2). The effect of smearing is not shown when it is smaller than the size of the symbols. Monte Carlo simulations suggest that the two data sets should collapse. The lack of agreement between simulation results and experiment is evident.

comment by Fredrickson and Helfand.[25] We therefore consider other explanations.

Comparison of Experiments with Monte Carlo Simulations

Binder and Fried have conducted two series of Monte Carlo simulations, one on symmetric diblock copolymers with $\phi = 0.5$,[26] and the other on asymmetric diblock copolymers with $\phi = 0.25$.[27] The study on asymmetric block copolymers is of particular interest because SI(4−13) and SI(8−22) have approximately the same composition. In the simulations, the repulsive interactions between the monomers of the two blocks were quantified by a dimensionless parameter, ϵ. Binder and Fried found that the simulated scattering data obtained from several different block copolymers with $\phi = 0.25$ collapsed on to a single curve when N/I_m was plotted as a function of ϵN. Since ϵ should scale as $1/T$,[25,26] we expected a collapse of the data when N/I_m is plotted as a function of N/T. In Figure 12 we show the data from SI(4−13) and SI(8−22) plotted in this manner. It is evident that our data are not consistent with the simulations of Binder and Fried.

Binder and Fried also found scaling laws for the dependence of q_m on T. They found that q_m changes more rapidly with temperatures as the ODT is approached. Their results suggest that $q_m N^{1/2}$ should scale with N/T. It is evident from the data shown in Figure 5 that these results are also inconsistent with our data. For copolymers with $0.25 < \phi < 0.5$ (only copolymers with $\phi = 0.5$ and $\phi = 0.25$ were studied by simulation), we find a linear dependence of q_m on T with a slope that was independent of composition, molecular weight, and proximity to the ODT. All observed deviations from linearity occurred in the vicinity of the glass transition temperature. However, the scattering profiles from such samples depend on thermal history[51] and are not discussed in this paper.

Scattering Profiles as the Order−Disorder Transition Is Approached

Bates et al.[52] and Winey et al.[53] demonstrated that the ODT is accompanied by an abrupt broadening of the small-angle scattering peak. The broadening can be identified by studying the scattered intensity at wave vectors greater than q_m as a function of temperature.[51−53] It was found that the scattering intensity at $q > q_m$ *increased* discontinuously at the ODT due to broadening of the scattering curve. In Figure 13 we plot $I(q)$ versus q obtained from SI(8−22). The curves obtained above 143 °C are broader than those obtained below 143 °C. In Figure 13 (inset) we plot $I(q=0.048\ \text{Å}^{-1})$ as a function of T and observe a discontinuity in the vicinity of the ODT determined by birefringence (145 ± 3 °C). All the polymers that showed a discontinuity in optical birefringence also showed an increase in the scattered intensity at $q > q_m$ at similar temperatures. In contrast, no such broadening was observed in the copolymers that were not birefringent in the observable temperature window. An example is shown in Figure 14, where the scattering data obtained from SI(6−10) at several temperatures are plotted. The intensity in the high-q regime—$I(q=0.061\ \text{Å}^{-1})$—shows no evidence of a transition.

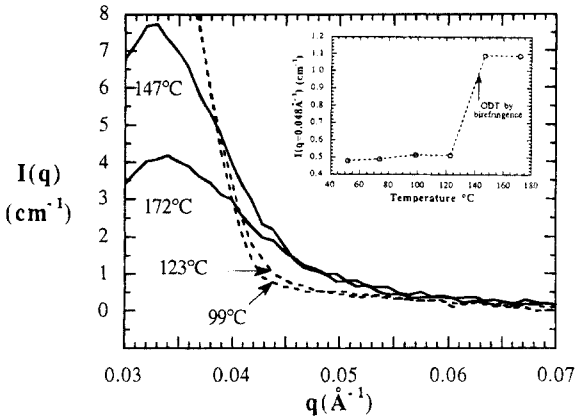

Figure 13. SANS profiles obtained from SI(8−22) at selected temperatures. The discontinuous increase in the intensity in the high-q regime ($q = 0.048\ \text{Å}^{-1}$) is evident due to broadening of the structure factor upon disordering (inset).

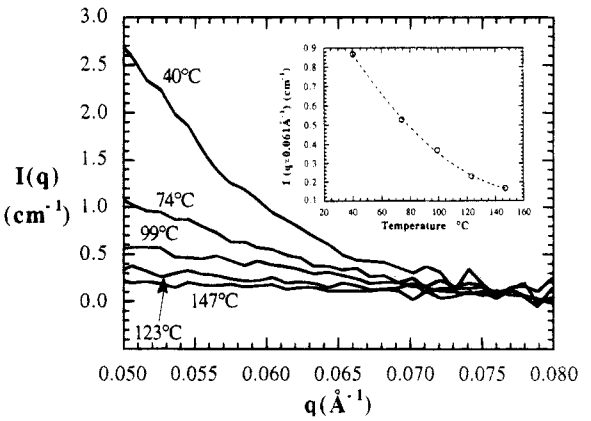

Figure 14. SANS profiles obtained from SI(6−10) at selected temperatures. Discontinuity is not observed in the high-q regime (inset), indicating that the sample is disordered in the experimentally available temperature window.

In Figure 15a we show how the mean-field χ parameters approach the spinodal value (ODT). The value of χ at the spinodal, χ_s, was evaluated by finding the point at which the mean-field prediction for $I(q_m)$ diverges. This requires some iteration because of the temperature dependence of the monomer volumes. The solid symbols represent the birefingence results with the mean-field interpretation, i.e., $\chi = \chi_s$ at the birefringence singularity. It is evident that the divergence of the small-angle scattering and the birefringence singularity occur at

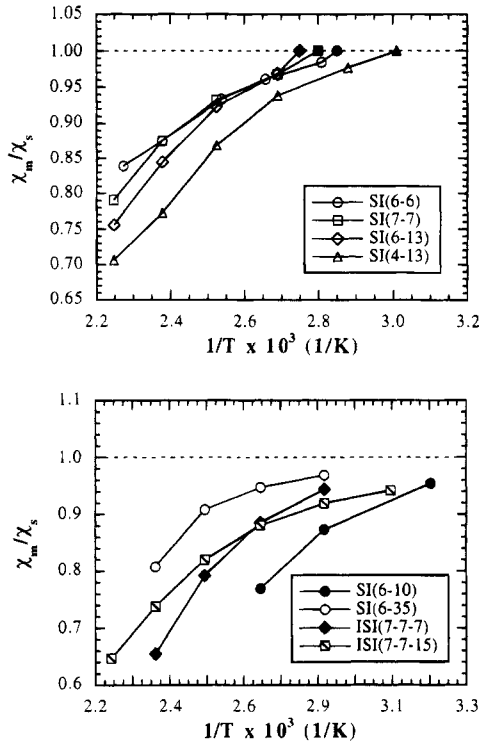

Figure 15. (a) Dependence of χ_m/χ_s, the ratio of the mean-field χ parameter at a given temperature to its value at the spinodal, on temperature. The solid symbols represent spinodal points determined from birefringence measurements. (b) Dependence of χ_m/χ_s, the ratio of the mean-field χ parameter at a given temperature to its value at the spinodal, on temperature for block copolymers that did not show a discontinuity in optical birefringence.

approximately the same temperature. Estimates of the spinodal temperature based on smooth extrapolations of the χ_m versus $1/T$ data to $\chi_m/\chi_s = 1$ would, however, lead to small errors. This was predicted by Fredrickson and Helfand on the basis of fluctuation effects.[25] We also see that the curvature in the χ_m versus $1/T$ data is a signature of the impending ODT, although the onset of the curvature occurs well before the transition.

In Figure 15b we plot χ_m/χ_s versus $1/T$ for systems which did not show a birefringence singularity. The curvature and the high values of χ/χ_s at the lower temperatures suggest that SI(6−35), SI(6−10), ISI(7−7−7), and ISI(7−7−15) are in the vicinity of the ODT.

In Figure 16 we show how the fluctuation-corrected χ parameters change with temperature as the ODT is approached. We plot χ_f/χ_t versus $1/T$ for the nearly symmetric diblock copolymers. The parameter χ_t is the value of χ_f at the ODT, which for $\phi = 0.46$ diblock copolymers is given by[10,25]

$$\chi_t N = 10.698 + 43.16(Nl^6/v^2)^{-1/3} \qquad (20)$$

In contrast to the mean-field results, the data shown in Figure 16 are reasonably consistent with a linear relationship between χ_f and $1/T$ up to the ODT.

In Figure 17, where we plot N/T versus ϕ, we show the phase diagram that we have obtained for polystyrene−polyisoprene diblock copolymers. Usually, the ordinate in block copolymer phase diagrams is χN.[2,25] We have chosen to replace χ with $1/T$ because of our inability to obtain a universal χ parameter that is consistent with all our data. The data points represent birefringence measurements except for $\phi = 0.13$, which is based on extrapolation of χ_m to the spinodal. We also

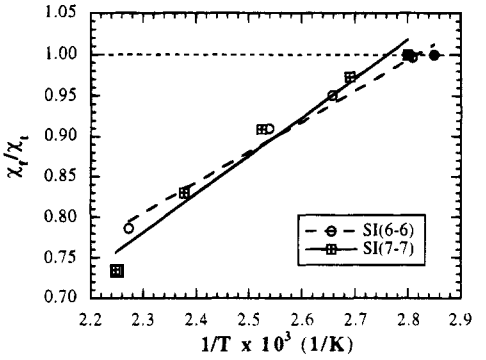

Figure 16. Dependence of χ_f/χ_t, the ratio of the fluctuation-corrected χ parameter at a given temperature to its value at the ODT, on temperature. The solid symbols represent the ODT points determined from birefringence measurements [circle, SI(6−6); square, SI(7−7)]. The lines represent least squares fits through χ_f/χ_t versus $1/T$ data. Intersections of these lines with $\chi_f/\chi_t = 1$ are in reasonable agreement with birefringence measurements.

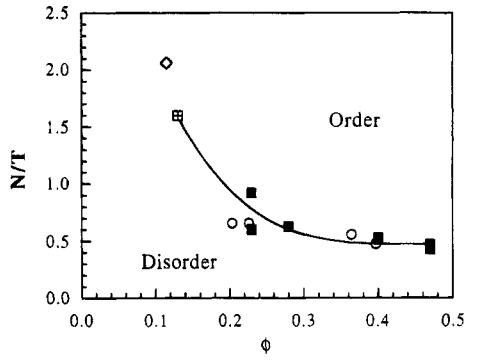

Figure 17. Phase diagram of polystyrene−polyisoprene diblock copolymers. Solid squares represent the birefringence results for the ODT, and the hatched square represents the estimated location of the mean-field spinodal for SI(6−35) based on an extrapolation of SANS data. The curve is meant to serve as an approximate border between order and disorder. Open circles and diamond are data from Winey et al.[53] and Adams et al.,[54] respectively.

show ODT data for SI polymers obtained by Winey et al.[52] and Adams et al.[54] The three sets of data are in reasonable agreement.

Concluding Remarks

We have conducted a systematic experimental study of linear polystyrene−polyisoprene block copolymer melts. The scattering profiles in the disordered state were measured by SANS. The main features of the scattering profiles, namely, the location of the scattering peak, q_m, and the height of the peak, I_m, were compared with the theoretical predictions of Leibler,[2] Fredrickson and Helfand,[25] and the simulations of Binder and Fried.[27] We found that the dependence of q_m on N and ϕ could be fit to a functional form suggested by Leibler over the entire experimental window. The dependence of I_m on N and ϕ was in reasonable agreement with the mean-field theory of Leibler as well as the fluctuation-based theory of Fredrickson and Helfand for block copolymers with $0.25 < \phi < 0.5$. However, for low molecular weight block copolymers with $\phi < 0.25$, we found anomalously high scattering peaks, indicating the presence of concentration fluctuations with unexpectedly large amplitudes. The scattered intensities at the peak from these asymmetric block copolymers were an order of magnitude greater than that expected from χ parameters obtained from symmetric block copolymers.

This trend cannot be explained by a composition-dependent χ parameter, because higher molecular weight block copolymers with the same asymmetry (ϕ) do not exhibit this anomaly. The observed effects are well outside expected uncertainties in polymer characterization, including polydispersity,[55] and in instrumentation (Appendix 2). We have used nondeuterated materials and thus do not have to consider complications arising from the effect of deuterium substitution on thermodynamics.[56-59]

The beauty of the RPA framework[1,2] is its simplicity and the ease with which it can be applied to mixtures with arbitrary complexity[3-6,33] such as asymmetric triblock copolymers. However, it is important to determine the limitations of this simple description and to develop frameworks with broader applicability if needed. Several attempts to go beyond RPA have been made.[25-27,60-63] The physical origin of some of our observations may be contained in these developments. For example, Semenov[63] predicts the formation of micelles in the disordered state of asymmetric block copolymers. The concentration and characteristics of the micelles were shown to depend on the χ parameter. The formation of such structures may produce the observed excess scattering. However, it is not possible to make quantitative estimates of this contribution, because of our inability to obtain a unique (composition and molecular weight independent) χ parameter for the interactions between the blocks. We could not compare our results with the simulations of Larson[62] for the same reason. The discussions in this paper are limited to theories that make direct predictions of the small-angle scattering profiles in disordered block copolymers. We found that none of these theories were entirely consistent with the data.

Acknowledgment. It is a pleasure to acknowledge Boualem Hammouda for teaching us about multicomponent RPA theories, Glenn Fredrickson for discussions on the fluctuation theory, John Barker for his help in estimating the effect of instrumental smearing, Lew Fetters for his help with polymer synthesis, and Charles Han for his help with the SANS experiments. We thank NIST for providing us with instrument time on the NG5 SANS machine. Financial support from the National Science Foundation through Grants CTS-9308164 and DMR-9307098 is gratefully acknowledged.

Appendix 1. Parameter Estimation for SANS Data Analysis

We have chosen to define the monomers in each block as the chemical repeat units, i.e., C_8 units for polystyrene and C_5 units for polyisoprene. The scattering lengths, b_i, and chain lengths, N_i, were estimated from characterization data. The monomer volumes, v_i, were calculated from densities and thermal expansion coefficients of the homopolymers, α_i, and were estimated as follows:

$$v_i = v_{i,0} \exp(-\alpha_i(T - 396)) \qquad (21)$$

where $v_{i,0}$ is the monomer volume at 396 K. Parameters common to all the block copolymers are listed in Table 2.

Other parameters required for the data analysis are listed in Table 3. Values of I_{inc} and l are weak functions of temperature. Only values at 123 °C are reported in Table 3. Methods used for estimating these parameters at other temperatures are given in the text.

Table 2. List of Parameters Common to All Block Copolymers

parameter	polystyrene	polyisoprene
b_i (Å)	2.32×10^{-4}	0.33×10^{-4}
$v_{i,0}$ (Å^3)	176.4	132.3
α_i (K^{-1})	5.5×10^{-4}	6.5×10^{-4}

Table 3. List of Parameters Used to Obtain χ_m and χ_f from SANS Data

		N_i		
polymer	I_{inc}[a] (cm^{-1})	PS block	PI block(s)	l[b] (Å^{-1})
SI(11-7)	1.07	108	97	8.4
SI(6-6)	1.05	62	95	8.1
SI(6-10)	1.00	54	145	7.6
SI(6-13)	1.00	56	190	8.0
SI(4-13)	1.02	40	185	7.9
SI(8-22)	1.02	75	328	8.2
SI(6-35)	0.98	58	519	8.3
SI(7-7)	1.05	69	106	8.3
ISI(7-7-7)	1.04	69	106 and 107	8.4
ISI(7-7-15)	1.06	69	106 and 228	9.2

[a] At 123 °C based on H atom concentration. See text for estimating I_{inc} at other temperatures. [b] At 123 °C by fitting SANS profiles. Values of l at other temperatures can be obtained from data given in Figure 5.

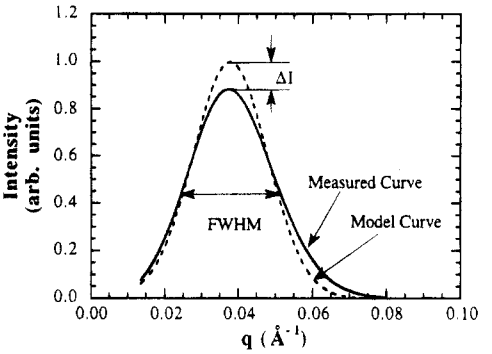

Figure 18. Effect of instrumental smearing on typical scattering profiles.

Appendix 2. Effect of Instrumental Smearing

The effect of instrumental smearing was estimated using a program provided by J. G. Barker of NIST.[64] Smearing effects due to collimation and finite size of the incident beam, wavelength spread, detector resolution and normalization, and circular averaging were estimated. Typical results for the instrument configuration specified in the Experimental Section are shown in Figure 18. The solid curve represents what would be measured if the "real" scattering curve was given by the dashed curve. Note that the peak width and position shown in Figure 18 are typical of our experimental data. It is evident that smearing had no effect on the peak position but results in a decrease in peak height by an amount ΔI, based on unit peak intensity, and a broadening of the peak resulting in a measured full width at half-maximum (fwhm) that is larger than the model curve. It is also evident that if the measured curve were shifted vertically so that the peak height was unity, then the "difference" between the model and measured curves would resemble the observed difference between experiment and the mean-field theory (see Figure 9a-c).

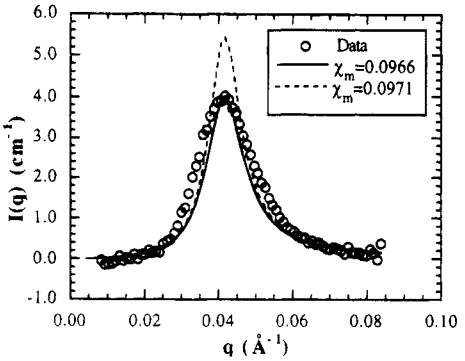

Figure 19. Corrections for instrumental smearing effects on data obtained from SI(4−13) at 75 °C. The estimated decrease in measured peak intensity due to instrumental smearing is 1.35 cm^{-1}. The χ_m value obtained from the measured data is 0.0966 while that obtained after smearing corrections is 0.0971.

We repeated such smearing estimations for several peak widths and obtained a relationship between ΔI and fwhm. Since smearing effects are most significant for sharp peaks, we have chosen to demonstrate smearing effects on data obtained from SI(4−13) at 75 °C, and the results are shown in Figure 19. For this case we estimate a 25% decrease in I_m due to smearing. The dashed curve in Figure 19 represents the mean-field theory with χ_m adjusted so as to match this estimated smearing effect. The value of χ_m obtained after desmearing was 0.0971, while that obtained from the measured data was 0.0966. The effect of smearing on χ and l is thus negligible (<1%). The values of χ_m and χ_f reported in this paper are thus based on measured data. However, when I_m values are reported, as in Figure 12, we present both unsmeared and measured values.

Appendix 3. Details Concerning the Estimation of χ_f

Following Fredrickson and Helfand[25] and Bates et al.,[10] x^* and $F(x^*,\phi)$ were obtained from Table 1 of ref 25 (ϕ in this paper is identical to f in refs 10 and 25), and C is given by

$$C = \{x^*F''(x^*,\phi)/3\}^{3/2}\{3x^*/2\pi\}\lambda(\phi) \qquad (22)$$

where x^*, $F''(x^*,\phi)$, and $\lambda(\phi)$ are also given in Table 1 of ref 25.

Nomenclature

b_i	scattering length of monomer i (i = A, B)
I	coherent SANS intensity (cm^{-1})
I_m	coherent SANS intensity at the peak (cm^{-1})
l	statistical segment length obtained by fitting SANS data to mean-field theory
l_i	statistical segment length of block i (i = A, B)
N	number of repeat units per chain based on reference volume v; $N = (N_A v_A + N_B v_B)/v$
N_i	number of monomers per block (i = A, B, 1, 2) (number of C_5 units in a polyisoprene block and number of C_8 units in a polystyrene block)
q	scattering vector (Å^{-1})
q_m	scattering vector at the peak (Å^{-1})
T	absolute temperature (K)
v	reference volume (=150.3 Å^3 throughout this paper)
v_i	volume of a monomer (i = A, B)
χ_f	fluctuation-corrected Flory−Huggins interaction parameter, based on v
χ_m	mean-field Flory−Huggins interaction parameter, based on v
χ_s	mean-field Flory−Huggins interaction parameter at the spinodal, based on v
χ_t	fluctuation-corrected Flory−Huggins interaction parameter at the ODT, based on v
ϕ	volume fraction of minor component in the block copolymer
ϕ_i	volume fraction of block i (i = A, B, 1, 2)

References and Notes

(1) de Gennes, P. G. *Scaling Concepts in Polymer Physics*; Cornell University Press: Ithaca, NY, 1979.
(2) Leibler, L. *Macromolecules* **1980**, *13*, 1602.
(3) de Gennes, P.-G. *Faraday Discuss. R. Soc. Chem.* **1979**, *68*, 96.
(4) Akcasu, A. Z.; Tombakoglu, M. *Macromolecules* **1990**, *23*, 607.
(5) Benoit, H.; Benmouna, M.; Wu, W. L. *Macromolecules* **1990**, *23*, 1511.
(6) Akcasu, A. Z.; Klein, R.; Hammouda, B. *Macromolecules* **1993**, *26*, 4136.
(7) Herkt-Maetzky, C.; Schelten, J. *Phys. Rev. Lett.* **1983**, *51*, 896.
(8) Hadziioannou, G.; Stein, R. S. *Macromolecules* **1984**, *17*, 567.
(9) Mori, K.; Hasegawa, H.; Hashimoto, T. *Polym. J.* **1985**, *17*, 799.
(10) Bates, F. S.; Rosedale, J. H.; Fredrickson, G. H. *J. Chem. Phys.* **1990**, *92*, 6255.
(11) Huggins, M. L. *J. Chem. Phys.* **1941**, *9*, 440.
(12) Flory, P. J. *J. Chem. Phys.* **1941**, *9*, 660.
(13) Han, C. C.; Bauer, B. J.; Clark, J. C.; Muroga, Y.; Matsushita, Y.; Okada, M.; Tran-Cong, Q.; Chang, T.; Sanchez, I. *Polymer* **1988**, *29*, 2002.
(14) Gehlsen, M. D.; Rosedale, J. H.; Bates, F. S.; Wignall, G. D.; Hansen, L.; Almdal, K. *Phys. Rev. Lett.* **1992**, *68*, 2452.
(15) Balsara, N. P.; Fetters, L. J.; Hadjichristidis, N.; Lohse, D. J.; Han, C. C.; Graessley, W. W.; Krishnamoorti, K. *Macromolecules* **1992**, *25*, 6137.
(16) Bates, F. S.; Muthukumar, M.; Wignall, G. D.; Fetters, L. J. *J. Chem. Phys.* **1988**, *89*, 535.
(17) Krishnamoorti, R.; Graessley, W. W.; Balsara, N. P.; Lohse, D. J. *J. Chem. Phys.* **1994**, *100*, 3894.
(18) Schweizer, K. S.; Curro, J. G. *J. Chem. Phys.* **1989**, *91*, 5059.
(19) Sariban, A.; Binder, K. *J. Chem. Phys.* **1987**, *86*, 5859.
(20) Hashimoto, T.; Mori, K. *Macromolecules* **1990**, *23*, 5347.
(21) Mori, K.; Tanaka, H.; Hasegawa, H.; Hashimoto, T. *Polymer* **1989**, *30*, 1389.
(22) Stuhn, B. *J. Polym. Sci., Polym. Phys. Ed.* **1992**, *30*, 1013.
(23) Balsara, N. P.; Lin, C. C.; Dai, H. J.; Krishnamoorti, R. *Macromolecules* **1994**, *27*, 1216.
(24) Owens, J. N.; Gancarz, I. S.; Koberstein, J. T.; Russell, T. P. *Macromolecules* **1989**, *22*, 3388.
(25) Fredrickson, G. H.; Helfand, E. *J. Chem. Phys.* **1987**, *87*, 697.
(26) Binder, K.; Fried, H. *J. Chem. Phys.* **1991**, *94*, 8349.
(27) Binder, K.; Fried, H. *Macromolecules* **1993**, *26*, 6878.
(28) Balsara, N. P.; Perahia, D.; Safinya, C. R.; Tirrell, M.; Lodge, T. P. *Macromolecules* **1992**, *25*, 3896.
(29) Balsara, N. P.; Garetz, B. A.; Dai, H. J. *Macromolecules* **1992**, *25*, 6072.
(30) Krishnamoorti, R. Ph.D. Thesis, Princeton University, 1993.
(31) Balsara, N. P.; Jonnalagadda, S. V.; Lin, C. C.; Han, C. C.; Krishnamoorti, R. *J. Chem. Phys.* **1993**, *99*, 10011.
(32) This procedure for estimating I_{inc} is only approximate due to well-known complexities associated with incoherent scattering described in: Maconnachie, A. *Polymer* **1984**, *25*, 1068. However, for rubbery hydrocarbon polymers with similar H atom concentrations, this method has proven to be adequate.[30]
(33) Hammouda, B. *Adv. Polym. Sci.* **1993**, *106*, 87.
(34) Mayes, A. M.; Olvera de la Cruz, M. *J. Chem. Phys.* **1989**, *91*, 7228.
(35) Mori, K.; Tanaka, H.; Hashimoto, T. *Macromolecules* **1987**, *20*, 381.
(36) Amundson, K. R.; Helfand, E.; Patel, S. S.; Quan, X.; Smith, S. S. *Macromolecules* **1992**, *25*, 1935.
(37) Garetz, B. A.; Newstein, M. C.; Dai, H. J.; Jonnalagadda, S. V.; Balsara, N. P. *Macromolecules* **1993**, *26*, 3151.
(38) Born, M.; Wolf, E. *Principles of Optics*; Pergamon: Oxford, U.K., 1959.

(39) Chung, C. I.; Gale, J. C. *J. Polym. Sci., Polym. Phys. Ed.* **1976**, *14*, 1149.
(40) Gouinlock, E. V.; Porter, R. S. *Polym. Eng. Sci.* **1977**, *17*, 535.
(41) Gehlsen, M. D.; Almdal, K.; Bates, F. S. *Macromolecules* **1992**, *25*, 939.
(42) Balsara, N. P.; Hammouda, B. *Phys. Rev. Lett.* **1994**, *72*, 360.
(43) Balsara, N. P.; Hammouda, B.; Kesani, P. K.; Jonnalagadda, S. V.; Straty, G. C. *Macromolecules* **1994**, *27*, 2566.
(44) Roe, R. J.; Fishkis, M.; Chang, J. C. *Macromolecules* **1981**, *14*, 1091.
(45) Fetters, L. J., private communication.
(46) Leibler, L.; Benoit, H. *Polymer* **1981**, *22*, 195.
(47) Benoit, H.; Wu, W.; Benmouna, M.; Mozer, B.; Bauer, B.; Lapp, A. *Macromolecules* **1985**, *18*, 986.
(48) Burger, C.; Ruland, W.; Semenov, A. N. *Macromolecules* **1990**, *23*, 3339.
(49) Brazovskii, S. A. *Sov. Phys.—JETP (Engl. Transl.)* **1975**, *41*, 85.
(50) Mayes, A. M.; Olvera de la Cruz, M. *J. Chem. Phys.* **1991**, *95*, 4670.
(51) Perahia, D.; Vacca, G.; Patel, S. S.; Dai, H. J.; Balsara, N. P., *Macromolecules* to appear.
(52) Bates, F. S.; Rosedale, J. H.; Bair, H. E.; Russell, T. P. *Macromolecules* **1989**, *22*, 2557.
(53) Winey, K. I.; Gobran, D. A.; Xu, Z.; Fetters, L. J.; Thomas, E. L. *Macromolecules* **1994**, *27*, 2392.
(54) Adams, J. L.; Graessley, W. W.; Register, R. A. *Macromolecules*, to appear.
(55) Using the results of Benoit et al.,[47] the value of χ_m obtained for SI(6−6) at 83 °C was 0.0646, assuming a polydispersity index of 1.05 for each block. The value of χ_m obtained for SI(6−6) at 83 °C ignoring polydispersity was 0.0677. The effect of polydispersity on χ_m of diblock copolymers is thus <3%. Polydispersity correction for triblock copolymers and χ_f is considerably more involved[48] and has not been carried out.
(56) Buckingham, A. D.; Hentschel, H. G. E. *J. Polym. Sci., Polym. Phys. Ed.* **1980**, *18*, 853.
(57) Bates, F. S.; Wignall, G. D.; Koehler, W. C. *Phys. Rev. Lett.* **1985**, *55*, 2425.
(58) Rhee, J.; Crist, B. *J. Chem. Phys.* **1993**, *98*, 4174.
(59) Graessley, W. W.; Krishnamoorti, R.; Balsara, N. P.; Fetters, L. J.; Lohse, D. J.; Schulz, D. N.; Sissano, J. A. *Macromolecules* **1993**, *26*, 1137.
(60) Melenkevitz, J.; Muthukumar, M. *Macromolecules* **1991**, *24*, 4199.
(61) Shull, K. *Macromolecules* **1992**, *25*, 2122.
(62) Larson, R. G. *Macromolecules*, in press.
(63) Semenov, A. N. *Macromolecules* **1989**, *22*, 2849.
(64) Barker, J. G.; Pederson, J. S., preprint.